文章编号：1000-7032(2016)02-0165-09

Synthesis of $AgNbO_3$/Graphene Nanocomposites with Highly Visible Light Photocatalytic Activity for Removal of Methyl Orange

MIAO Hui[1,2,3], XIA Juan[1], JIN Feng[1,2], SUN Lin[1,2],
CUI Yu-min[1,2*], LI Hui-quan[1,2], DING Jian[1]

(1. *School of Chemistry and Materials Engineering, Fuyang Normal College, Fuyang* 236037, *China*;
2. *Anhui Province Key Laboratory for Degradation and Monitoring of Pollution of The Environment, Fuyang* 236037, *China*;
3. *Key Laboratory of Functional Molecular Solids, Ministry of Education, Wuhu* 241000, *China*)

* *Corresponding Author, E-mail: cymlh@126.com*

Abstract: $AgNbO_3$/graphene nanocomposites were synthesized *via* the technique of solid-solid grinding and subsequent sintering process. Surface structures and optical properties of the prepared materials were characterized by transmission electron microscopy and UV-Vis diffuse reflection spectroscopy. The results indicate that band-gap of $AgNbO_3$ is lowered upon compositing with graphene nanoparticles, thereby giving an absorption in a large range of wavelengths. Degradation of methyl orange (MO) is carried out to evaluate the photocatalytic activity of $AgNbO_3$/graphene nanocomposites under visible light irradiation. Compared with pure $AgNbO_3$, $AgNbO_3$/graphene composites exhibit significantly enhanced photocatalytic activity for MO. Moreover, $AgNbO_3$/graphene (2∶1) obtained at 300 ℃ exhibits the highest degradation degree of MO after an irradiation of 120 min with apparent k_{app} of 0.034 min^{-1}, which is about 10 times than that of the pure $AgNbO_3$. The tests of radical scavengers confirm that $\cdot O_2^-$ and h^+ are the main reactive species for the degradation of MO.

Key words: solid-state method; $AgNbO_3$/graphene nanocomposites; photocatalysis; degradation; methyl orange
CLC number: O634 **Document code**: A **DOI**: 10.3788/fgxb20163702.0165

$AgNbO_3$/石墨烯复合材料的合成及其可见光催化甲基橙降解活性

苗 慧[1,2,3], 夏 娟[1], 金 凤[1,2], 孙 林[1,2], 崔玉民[1,2*], 李慧泉[1,2], 丁 建[1]

(1. 阜阳师范学院 化学与材料工程学院, 安徽 阜阳 236037; 2. 安徽环境污染物降解与监测省级实验室, 安徽 阜阳 236037;
3. 功能性分子固体省部共建教育部重点实验室, 安徽 芜湖 241000)

摘要: 采用固相法合成 $AgNbO_3$/石墨烯复合纳米材料,利用透射电子显微镜(TEM)及紫外-可见漫反射光谱(UV-Vis)对样品的形貌及光学性质进行了表征。研究发现,$AgNbO_3$ 与石墨烯复合后,带隙能明显降低,吸收光波长范围增大。以甲基橙溶液的降解为光催化模型反应评价了 $AgNbO_3$/石墨烯复合纳米材料的可见光催化性能。结果表明:与纯 $AgNbO_3$ 相比,$AgNbO_3$/石墨烯复合纳米材料对甲基橙的可见光催化性能明显增强。

收稿日期: 2015-09-14; **修订日期**: 2015-09-30
基金项目: 国家自然科学基金(21402029,21401024); 安徽省高校青年人才基金(2013SQRL058ZD); 安徽省自然科学基金(1408085MB35); 安徽省高校自然科学基金(KJ2014A191)资助项目

实验条件下,经300 ℃煅烧的$AgNbO_3$/石墨烯(2∶1)复合纳米材料表现出最优的催化性能,它对甲基橙的可见光催化脱色速率系数约为纯$AgNbO_3$的10倍。光催化降解机理研究表明,促使甲基橙降解脱色的主要活性物种为·O_2^-和h^+。

关 键 词:固相法;$AgNbO_3$/石墨烯纳米材料;可见光催化;降解;甲基橙

1 Introduction

Over the past few years, much attention has been paid to photocatalysis due to its potential application in removing environmental pollutants and converting solar energy[1-5]. Also, a number of photocatalysts with excellent photocatalytic efficiency and good stability have been developed, such as doped TiO_2[6], Bi_2WO_6[7], $CaBi_2O_4$[8] and Ag-based compounds[9]. Among this photocatalysts, silver niobate ($AgNbO_3$) discovered by Ye[10] and coworkers is regarded as a significant breakthrough in the field of visible light-driven photocatalyst. Although it exhibits excellent photo-oxidative capability for O_2 evolution from water splitting as well as highly efficient organic molecule decomposition activity under visible light[11-13], high photocatalytic activity for decomposition of organic pollutants still has not been achieved. It constitutes a challenge: how to improve the photocatalytic activity of $AgNbO_3$.

Graphene, a new crystalline form of carbon, not only possesses stable structure but also exhibits high specific surface area, and excellent electronic conductivity[14-17]. It has attracted tremendous scientific interest in many area, such as catalysis, luminescence and energy storage[18-20]. Recently, there have been extensively studies in the use of metal oxides/grapheme nanocomposites at photocatalysis and performed high activities[21-23]. Therefore, it is desirable to explore a simple and effective approach for constructing $AgNbO_3$/graphene composites and examine their practical application in photocatalytic degradation organic pollutants.

Herein, a facile strategy was developed to fabricate the $AgNbO_3$/graphene nanostructure composites by a solid method. On testing them in photocatalysis, our data demonstrated that the $AgNbO_3$/graphene materials exhibited excellent photocatalytic efficiency for the degradation of methyl orange (MO) under visible light irradiation. Especially, the $AgNbO_3$/graphene (2∶1) composite obtained at 300 ℃ showed the highest photocatalytic degradation performance for MO (CR) (>98%), which should be attributed to the extended optical absorption in visible light region. Moreover, the possible mechanism for dyes degradation over $AgNbO_3$/graphene composite was proposed. It can be predicted that this organic-inorganic hybrid material will have promising application in the photocatalysis filed in the future.

2 Experiments

2.1 Materials

All the chemicals were of analytical grade and used without further purification. Potassium permanganate ($KMnO_4$), hydrogen peroxide (H_2O_2), concentrated sulfuric acid (H_2SO_4), hydrochloric acid (HCl), hydrazine, silver nitrate ($AgNO_3$), phosphorus pentoxide (P_2O_5), potassium persulfate ($K_2S_2O_8$), niobium pentoxide (Nb_2O_5), the deionized water used throughout the whole experiments.

2.2 Synthesis of $AgNbO_3$/Graphene Nanocomposites

The $AgNbO_3$ was prepared by grinding the mixture of $AgNO_3$ (0.169 g, 1.0 mmol) and Nb_2O_5 (0.133 g, 0.5 mmol) for 30 min with an agate mortar and pestle at room temperature first and then sintering at 880 ℃ for 5 h in a muffle furnace. The graphene oxide was obtained according to the method of Hummers[20].

A series of solid $AgNbO_3$/graphene nanocomposites were prepared according to the following method: $AgNbO_3$ (0.124 g, 0.5 mmol) and graphene oxide (0.062 g) were mixed together and grinding for 30 min at room temperature. Then, a black product named $AgNbO_3$/graphene oxide-2 (the initial molar ratio of $AgNbO_3$ to graphene oxide

is 2∶1) was obtained. The other $AgNbO_3$/graphene oxides were also prepared as the same method but with different initial molar ratios of $AgNbO_3$ to graphene oxide. The $AgNbO_3$/graphene composites were obtained by sintering the $AgNbO_3$/graphene oxide-2 at different temperature for 5 h. All the materials obtained before analysis were kept in a vacuum desiccator over activated silica gel.

2.3 Photocatalysis of $AgNbO_3$/Graphene Nanocomposites

MO degradation measurements were performed in the presence of different $AgNbO_3$/graphene composites. $AgNbO_3$/graphene composite (40.0 mg) was added to the MO solution (40 mL, 40.00 mg · L^{-1} in distilled water) and magnetically stirred in the dark for 1.0 h to ensure the adsorption/desorption equilibrium of the solution with the photocatalyst. Subsequently, the solution was placed in an internal-irradiation quartz reaction cell (50.0 mL), and irradiated under visible light for 2 h. And then, for each 30 min interval, the top solution (4.5 mL) was collected for the measurement of UV-Vis spectroscopy with a wavelength range from 190 to 700 nm to determine the content of MO in the solution.

2.4 Instruments and Measurements

Transmission Electron microscopy (TEM) images were recorded by using a Jeol JEM-2100F microscope. UV-Vis diffuse reflection spectroscopy (DRS) of the samples were determined with a Shimadzu UV-3600 spectro photometer. UV-Vis absorption spectra were taken on a TU-1901 spectrometer over the wavelength range from 190 to 700 nm, using quartz cells with a 1 cm optical path at room temperature.

3 Results and Discussion

3.1 TEM

The morphology and microstructure of the as-prepared composites were characterized by TEM as shown in Fig. 1. As seen from TEM images, two kinds of $AgNbO_3$/graphene (2∶1) nanocomposites obtained at 300 and 500 ℃ were successfully fabricated using a solid-solid procedure. From Fig. 1(a), it can be seen that after sintering at 300 ℃, the $AgNbO_3$ nanoparticles with the size of about 10 – 20 nm were uniformly distributed on 2D graphene sheets. The $AgNbO_3$ nanoparticles, acting as spacers, can efficiently prevent the closely restacking of graphene sheets on the surface, avoiding the loss of their high active surface. In comparison with the nanocomposite obtained at 300 ℃, the size of $AgNbO_3$ nanoparticles in the $AgNbO_3$/graphene nanocomposite (2∶1, 500 ℃) had increased to large sizes of 30 – 50 nm. At the same time, the $AgNbO_3$ nanoparticles tend to agglomerate to larger cluster, which may affect the performance of the composite. It is likely that 300 ℃ seems to be the optimum temperature for the formation of the nanocomposite, DRS analysis of the material supports this point.

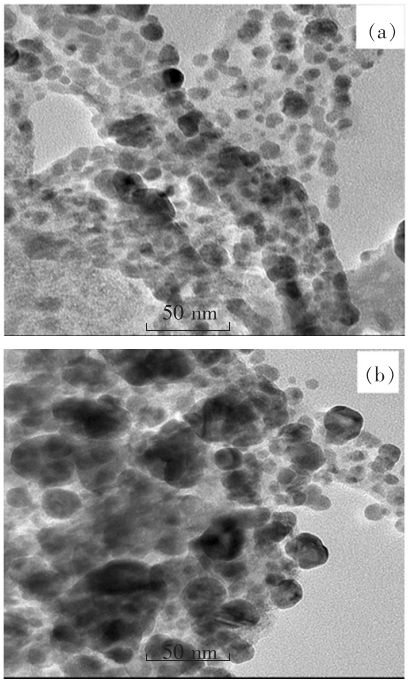

Fig. 1　TEM images of the obtained $AgNbO_3$/graphene (2∶1) nanocomposites obtained at 300 ℃ (a) and 500 ℃ (b)

3.2 DRS

It is well known that optical absorption property, a key factor in determining the photocatalytic performance of the catalyst, can exhibit the absorbed spectrum range of the catalyst[24]. To examine the optical absorption properties of $AgNbO_3$/graphene (2∶1) nanocomposites as well as $AgNbO_3$, we performed UV-Vis diffuse reflectance spectrum experiments (DRS). Fig. 2(A) shows the DRS of $AgNbO_3$ and $AgNbO_3$/graphene (2∶1) nanocomposites obtained

after sintering at 300, 400, 500, and 700 ℃. The obtained $AgNbO_3$ exhibited photo-absorption up to 450 nm, implying its visible light induced photocatalytic activity. Compared to the pure $AgNbO_3$, all of the composites showed stronger photo-absorption abilities in the visible light region, with the obvious longer wavelength shift of the absorption edges, indicating the more produced electron-hole pairs under the same visible light irradiation, which could result in higher photocatalytic performance. Meanwhile, the photo-absorption intensities of the composites were found to gradually decrease with the increasing sintering temperatures. It also suggested that the presence of graphene may be used as a means to reduce the band-gap of $AgNbO_3$, thereby giving an absorption in a large range of wavelengths.

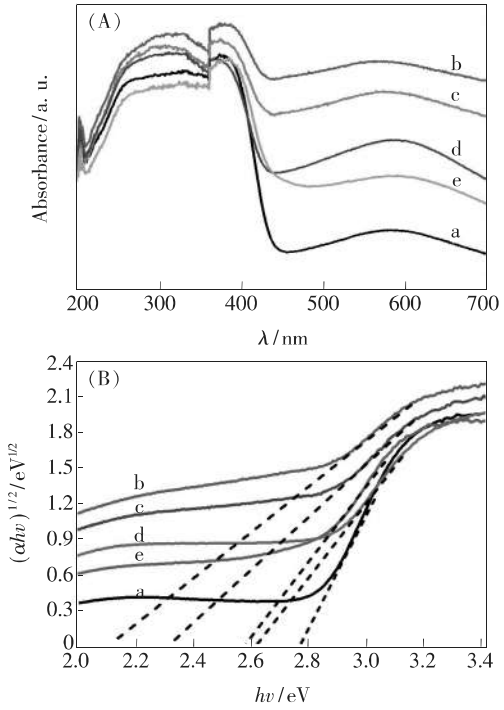

Fig. 2 (A) DRS spectra of $AgNbO_3$ (a) and $AgNbO_3$/graphene (2∶1) nanocomposites obtained at 300, 400, 500, and 700 ℃ (b, c, d, and e). (B) $(\alpha hv)^{1/2}$ *versus* hv plots of the materials.

According to the Kubelka-Munk function[25], the relation between absorption coefficient and the band-gap energy of a crystalline semiconductor can be described using the formula (1):

$$\alpha hv = A(hv - E_g)^{n/2}, \qquad (1)$$

where α, v, E_g and A are the absorption coefficient, light frequency, band-gap energy, and a constant, respectively. The band-gap energies (E_g) of $AgNbO_3$ and $AgNbO_3$/graphene nanocomposites could be estimated from a plot of $(\alpha hv)^{1/2}$ *versus* hv, as shown in Fig. 2(B). E_g of the pure $AgNbO_3$ was estimated to be 2.77 eV using the formula, which was similar to the reported value[26]. In addition, E_g values were about 2.62, 2.58, 2.32, and 2.11 eV for $AgNbO_3$/graphene (2∶1) nanocomposites obtained at 500, 700, 400, and 300 ℃, respectively. The relatively narrow band-gap energy observed for $AgNbO_3$/graphene (2∶1) nanocomposites may be ascribed to the strong interaction in the hybrid structure[27], which made the utilization of the solar energy more efficiently. Based on the results of the DRS and E_g values, we think that 300 ℃ is the optimum temperature for the formation of the $AgNbO_3$/graphene (2∶1) nanocomposites.

3.3 Photocatalytic Activity

The photocatalytic activities of the $AgNbO_3$/graphene composites were investigated by degrading MO in an aqueous solution under visible light irradiation. Fig. 3(a) revealed the variation of MO concentration (C/C_0) in the present of $AgNbO_3$/graphene oxide (GO) composites containing different concentrations of GO as well as pure $AgNbO_3$ during the same photodegradation time. All the $AgNbO_3$/GO composites exhibited higher photocatalytic activities than that of pure $AgNbO_3$. Further, with the increase of the content of GO from 20% to 50%, the photocatalytic activities of the MO solutions enhanced gradually and then decreased. The highest photocatalytic activity was achieved in the present of the $AgNbO_3$/GO (2∶1) composite. That is why we choose the $AgNbO_3$/GO (2∶1) composite as the precursor to obtain $AgNbO_3$/graphene (2∶1) composite.

Based on the above results, the photocatalytic properties of $AgNbO_3$/graphene (2∶1) nanocomposites obtained at 200, 300, 400, and 500 ℃ were evaluated and illustrated in Fig. 3(b). Initially, the photocatalytic activity quickly increased with the increase of the sintering temperatures from 200 to 300 ℃. Subsequently, as the sintering temperatures

increases further, the photocatalytic activity of the composites decreased slightly. The highest photocatalytic activity was achieved in the present of the $AgNbO_3$/graphene (2∶1) nanocomposite (300 ℃), at which 98.7% of MO was decomposed after 120 min irradiation. These data provided strong evidence that the photocatalytic activity of the $AgNbO_3$/graphene composite was not only mediated by the presence of graphene oxide, but also directly related to the sintering temperature of the composite. This result suggested an important clue to the possible significance of doped graphene in modifying the photocatalytic behavior of the $AgNbO_3$.

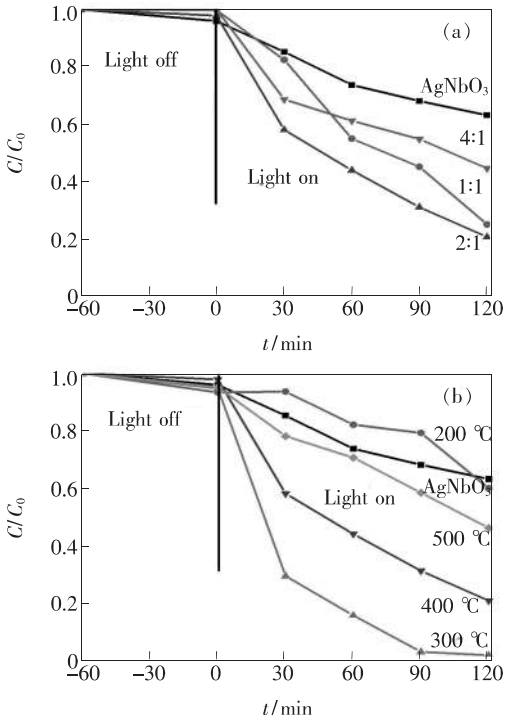

Fig. 3　(a) Photocatalytic activities of $AgNbO_3$ and $AgNbO_3$/GO composites on the degradation of MO under visible light irradiation. (b) Photocatalytic activities of $AgNbO_3$ and $AgNbO_3$/graphene composites obtained at 200, 300, 400, and 500 ℃ on the degradation of MO under visible light irradiation.

It is well known that photocatalytic oxidation of organic pollutants follows first-order kinetics[28]. The linear relationship between $\ln(C_0/C)$ and t shown in Fig. 4 confirms that the photocatalytic degradation process of MO followed the apparent pseudo-first-order model expressed as Eq. (2)[29-30].

$$\ln(C_0/C) = k_{app}t, \qquad (2)$$

Where C_0 is the initial concentration of MO solution ($mg \cdot L^{-1}$), C is MO concentration at time t ($mg \cdot L^{-1}$), k_{app} is the apparent pseudo-first-order rate constant (min^{-1}). Clearly, $AgNbO_3$/graphene (2∶1) nanocomposite (300 ℃) possessed the fastest degradation rate for MO with k_{app} value of 0.034 min^{-1} and was 10 times that of pure $AgNbO_3$ (k = 0.003 min^{-1}), which further confirmed the activity enhancement of $AgNbO_3$/graphene (2∶1) nanocomposite (300 ℃). The present results further support the fact that 300 ℃ is the optimum temperature for the formation of the nanocomposite.

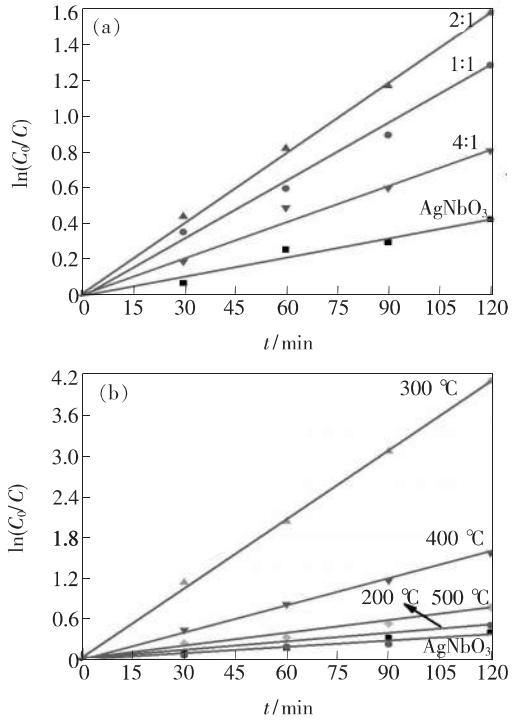

Fig. 4　(a) Linear transform $\ln(C_0/C) = f(t)$ of the kinetic curves of $AgNbO_3$ and $AgNbO_3$/GO composites. (b) Linear transform $\ln(C_0/C) = f(t)$ of the kinetic curves of $AgNbO_3$ and $AgNbO_3$/graphene composites obtained at 200, 300, 400, and 500 ℃ on the degradation of MO.

Furthermore, the absorption curves of MO in aqueous solutions kept for 2 h under visible light irradiation were displayed in Fig. 5. MO dye has its own maximum absorbance at 466 nm, which is in agreement with the literature[31]. Apparently, the introduction of $AgNbO_3$/graphene nanoparticles (2∶1, 300 ℃) leads to more obviously decrease of the intensity of the maximum absorption peaks than pure

$AgNbO_3$ catalyst after visible light irradiation, indicating that the $AgNbO_3$/graphene composite exhibited excellent photocatalytic activity for MO decomposition under visible light. This result was similar to the DRS analysis above.

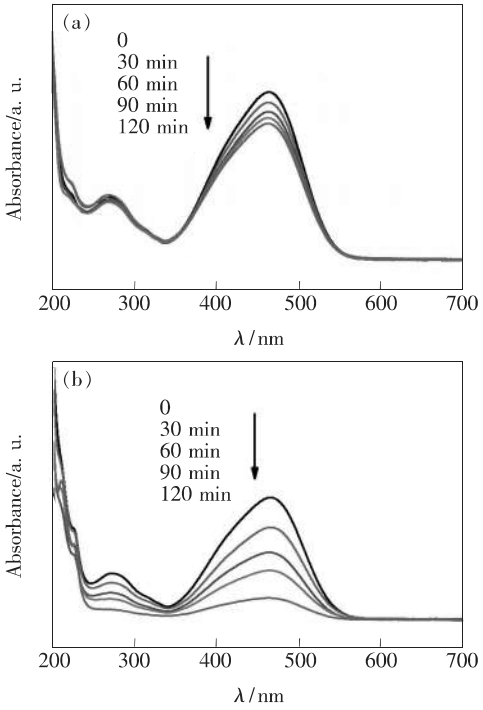

Fig. 5 UV-Vis spectra of the MO aqueous solution under visible light irradiation in the presence of $AgNbO_3$ and $AgNbO_3$/graphene (2∶1, 300 ℃) nanocomposite catalysts

3.4 Discussion of Photocatalytic Mechanism

3.4.1 Reactive Species Involved in The Photocatalytic Process

The effect of various radical scavengers on the degradation of MO over $AgNbO_3$/graphene (2∶1, 300 ℃) under visible light irradiation was performed to investigate the underlying photo-degradation mechanism. In the photocatalytic process, superoxide radicals ($\cdot O_2^-$), hydroxyl radicals ($\cdot OH$) and active holes (h^+) are often believed to be responsible for the photodegradation of organic pollutants[32-35]. In order to study which of these species are involved in MO degradation, it is necessary to clarify main active species for the photodegradation of MO. The radical scavengers isopropanol (IPA), benzoquinone (BQ), ammonium oxalate (AO), catalase (CAT) and NO_3^- ions were respectively used as the scavengers of $\cdot OH$, $\cdot O_2^-$, h^+, H_2O_2 and e_{cb}^-, respectively.

From the results shown in Fig. 6, it can be seen that different scavengers may produce different effects on the photocatalytic property of MO. It is clearly that the degradation ratio of MO was markedly reduced to 16.0% by the addition of AO, followed by BQ (24.0%) and IPA (61.2%), respectively. These degradation ratios were on average 3.88, 2.60, and 1.02-fold smaller than the result obtained in the absence of any scavenge. Unlike AO scavenger, the CAT or NO_3^- scavengers indicated a slight increase of the degradation ratios of MO. Therefore, we suggested that $\cdot OH$, h^+ and $\cdot O_2^-$, especially h^+, played crucial roles in the MO degradation process.

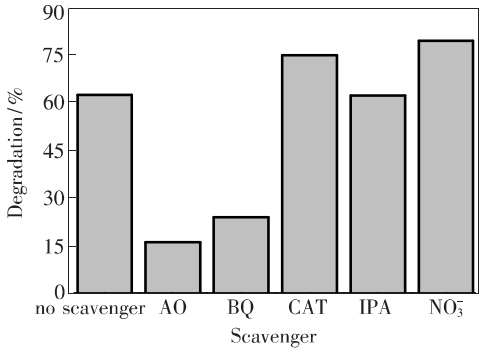

Fig. 6 Effects of different scavengers on the degradation of MO over $AgNbO_3$/graphene (2∶1, 300 ℃) nanocomposite under visible light irradiation

3.4.2 Origin of Reactive Species for MO Degradation

In addition, based on the above discussion of reactive species involved in the MO degradation, a possible pathway for the photocatalytic degradation of MO can be proposed as following Eqs. (3) – (12):

$$\text{Catalyst} + h\nu \rightarrow e_{cb}^- + h_{vb}^+, \quad (3)$$

$$e_{cb}^- + O_2 \rightarrow \cdot O_2^-, \quad (4)$$

$$e_{cb}^- + \cdot O_2^- + 2H^+ \rightarrow H_2O_2, \quad (5)$$

$$H_2O_2 + e_{cb}^- \rightarrow \cdot OH + OH^-, \quad (6)$$

$$H_2O_2 + h\nu \rightarrow 2 \cdot OH, \quad (7)$$

$$H_2O + h_{vb}^+ \rightarrow \cdot OH + H^+, \quad (8)$$

$$OH^- + h_{vb}^+ \rightarrow \cdot OH, \quad (9)$$

$$MO + \cdot OH \rightarrow \text{products}, \quad (10)$$

$$MO + \cdot O_2^- \rightarrow \text{products}, \quad (11)$$

$$MO + h_{vb}^+ \rightarrow \text{products}. \quad (12)$$

Here, we would like to present a possible degradation process of the dye to explain the improved photocatalytic activity in terms of our data. As illustrated in Fig. 7, under visible light irradiation, the $AgNbO_3$ in the composite was photo-excited to generate electrons in the conduction band (CB) and holes in the valence band (VB, Eq. (3)). The exited valence electrons quickly transferred to graphene from $AgNbO_3$, thereby causing electron accumulation at graphene interfaces. This process was beneficial to the separation of electron-hole pairs. Highly active oxidants such as $\cdot O_2^-$ and $\cdot OH$ were produced from oxygen by the photo-induced electrons on the graphene (Eqs. (4) – (6)). Meanwhile, the holes can further reacted with the adsorbed H_2O or OH^- on the surface of catalyst to form $\cdot OH$ (Eqs. (7) – (9)). The dye molecules were reacted with the active $\cdot O_2^-$, $\cdot OH$ and h^+ and degraded into s mall molecules such as CO_2 and H_2O (Eqs. (10) – (12)) through the direct oxidation and reduction reactions of MO by these active species. Undoubtedly, the synergetic effect of $AgNbO_3$ and graphene in electron transfer was a key factor for the improved photocatalytic activity. In addition, the strong adsorption ability of graphene and the relative narrow band-gap of the composite were also beneficial to the enhanced photocatalytic activity of the $AgNbO_3$/graphene composite.

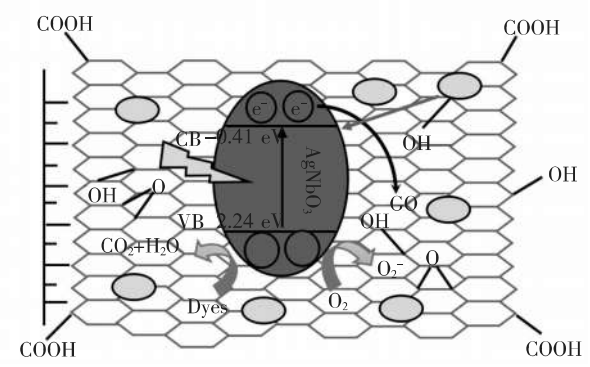

Fig. 7　Proposed mechanism for the photodegradation of organic molecules on the surface of $AgNbO_3$/graphene nanocomposite

4　Conclusion

In summary, the $AgNbO_3$/graphene nanocomposites were successfully fabricated through a facile one-step solid phase synthesis method. Importantly, the structure and band-gap energy of the composites can be tuned by adjusting the sintering temperatures. Further, the obtained $AgNbO_3$/graphene nanoparticles (2∶1, 300 ℃) material exhibited the highest photocatalytic activity for MO, with the degradation rate of 98.7% after 120 min irradiation, which was far better than those of pure $AgNbO_3$. This improved photocatalytic performance was attributed to the synergetic effect of $AgNbO_3$ and graphene in electron transfer, the strong adsorption ability of graphene and the relative narrow band-gap of the composite. Overall, this work represents an important step toward the $AgNbO_3$/graphene nanocomposite materials and the development of controllable synthesis of micro/nanostructures.

References:

[1] LANG X J, CHEN X D, ZHAO J C. Heterogenerous visible light photocatalysis for selective organic transformations [J]. *Chem. Soc. Rev.*, 2014, 43:473-486.

[2] FRESNO F, PORTELA R, SUAREZ S, *et al*.. Photocatalytic materials: recent achievements and near future trends [J]. *J. Mater. Chem.*, 2014, A2:2863-2884.

[3] XU Z K, HAN L, HUA P, *et al*.. Facile synthesis of small Ag@ AgCl nanoparticles *via* a vapor diffusion strategy and their highly efficient visible-light-driven photocatalytic performance [J]. *Catal. Sci. Technol.*, 2014, 4:3615-3619.

[4] SHI H X, LI G Y, SUN H W, *et al*.. Visible-light-driven photocatalytic inactivation of E. coli by Ag/Ag*X*-CNTs (*X* = Cl, Br, I) plasmonic photocatalysts: bacterialperformance and deactivation mechanism [J]. *Appl. Catal.* B, 2014, 158-159:301-307.

[5] 翟英娇,李金华,陈新影,等. 镉掺杂氧化锌纳米花的制备及其光催化活性 [J]. 中国光学, 2014, 7(1):124-130.
ZHAI Y J, LI J H, CHEN X Y, *et al*.. Synthesis and characterization of Cd-doped ZnO nanoflowers and its photocatalytic

activity [J]. *Chin. Opt.*, 2014, 7(1):124-130. (in Chinese)

[6] SCHNEIDER J, MATSUOKA M, TAKEUCHI M, *et al.*. Understanding TiO_2 photocatalysis: mechanisms and materials [J]. *Chem. Rev.*, 2014, 114:9919-9986.

[7] TAMAR S, PIERRE G, NICOLAS C, *et al.*. New Insights into Bi_2WO_6 properties as a visible-light photocatalyst [J]. *J. Phys. Chem.* C, 2013, 117:22656-22666.

[8] TANG J W, ZOU Z G, YE J H. Efficient photocatalytic decomposition of organic contaminants over $CaBi_2O_4$ under visible light irradiation [J]. *Angew. Chem. Int. Ed.*, 2004, 43:4463-4466.

[9] CHEN Z H, BING F, LIU Q, *et al.*. Novel Z-scheme visible-light-driven Ag_3PO_4/Ag/SiC photocatalysts with enhanced photocatalytic activity [J]. *J. Mater. Chem.* A, 2015, 3:4652-4658.

[10] YI Z G, YE J H, KIKUGAWA N, *et al.*. An orthophosphate semiconductor with photooxidation properties under visible-light irradiation [J]. *Nat. Mater.*, 2010, 9:559-564.

[11] BELEN J A, MARTIN D J, DHANOA M T, *et al.*. H_2 and O_2 evolution from water half-splitting reactions by graphitic carbon nitride materials [J]. *J. Phys. Chem.* C, 2013, 117:7178-7185.

[12] BI Y P, OUYANG S X, UMEZAWA N T, *et al.*. Facet effect of single-crystalline Ag_3PO_4 submicro-crystals on photocatalytic properties [J]. *J. Am. Chem. Soc.*, 2011, 133:6490-6492.

[13] LIU Y P, FANG L, LU H D, *et al.*. Highly efficient and stable Ag/Ag_3PO_4 plasmonic photocatalyst in visible light [J]. *Catal. Commun.*, 2012, 17:200-204.

[14] SHOWN I, HSU H C, CHANG Y C, *et al.*. Highly efficient visible light photocatalytic reduction of CO_2 to hydrocarbon fuels by Cu-nanoparticle decorated graphene oxide [J]. *Nano. Lett.*, 2014, 14:6097-6103.

[15] LIANG J B, WANG Z M, SUN M C, *et al.*. Synergetic photocatalysts derived from porous organo Ti-O clusters pillared graphene oxide frameworks (GOFs) [J]. *RSC Adv.*, 2014, 4:60729-60732.

[16] DR TIRTHA S, GERALD V T, ROBERT W, *et al.*. Graphene oxide/α-Bi_2O_3 composites for visible-light photocatalysis, chemical catalysis, and solar energy conversion [J]. *ChemSusChem*, 2014, 7:854-865.

[17] LIANG Y Y, LI Y G, WANG H L, *et al.*. Co_3O_4 nanocrystals on graphene: a synergetic catalyst for oxygen reduction reaction [J]. *Nat. Mater.*, 2011, 10:780-786.

[18] WANG J, GAO Z, LI Z S, *et al.*. Green synthesis of graphene nanosheets/ZnO composites and electrochemical properties [J]. *J. Solid. State. Chem.*, 2011, 184:1421-1427.

[19] YANG Y, REN L L, ZHANG C, *et al.*. Facile fabrication of functionalized graphene sheets (FGS)/ZnO nanocomposites with photocatalytic property [J]. *Appl. Mater. Interf.*, 2011, 3:2779-2785.

[20] JIANG G D, LIN Z F, CHEN C, *et al.*. TiO_2 nano-particles asse MO led on graphene oxide nanosheets with high photocatalytic activity for removal of pollutants [J]. *Carbon*, 2011, 49:2693-2701.

[21] PEI F, LIU Y, XU S, *et al.*. Nanocomposite of graphene oxide with nitrogen-doped TiO_2 exhibiting enhanced photocatalytic efficiency for hydrogen evolution [J]. *Int. J. Hydrogen Energy*, 2013, 38:2670-2677.

[22] ZENG J, WANG H, ZHANG Y C, *et al.*. Hydrothermal synthesis and photocatalytic properties of pyrochlore $La_2Sn_2O_7$ nanocubes [J]. *J. Phys. Chem.* C, 2007, 111:11879-11887.

[23] KIM Y K, MIN D H. UV protection of reduced graphene oxide films by TiO_2 nanoparticle incorporation [J]. *Nanoscale*, 2013, 5:3638-3642.

[24] WILLIAMS G, SEGER B, KAMAT P V. TiO_2-graphene nanocomposites UV-assisted photocatalytic reduction of graphene oxide [J]. *ACS Nano*, 2008, 2:1487-1491.

[25] LI Y Y, LIU J P, HUANG X T, *et al.*. Carbon-modified Bi_2WO_6 nanostructures with improved photocatalytic activity under visible light [J]. *Dalton Trans.*, 2010, 39:3420-3425.

[26] LI Y, LI X, LI J, *et al.*. Photocatalytic degradation of MO by TiO_2 coated activated carbon and kinetic study [J]. *Water Research*, 2006, 40:1119-1126.

[27] Sun J H, Wang X L, Sun J Y, *et al.*. Photocatalytic degradation and kinetics of orange G using nanosized Sn(IV)/TiO_2/AC photocatalyst [J]. *J. Mol. Catal.* A, 2006, 260:241-246.

[28] WU C H, CHANG H W, CHEN J M. Basic dye decomposition kinetics in photocatalytic slurry reactor [J]. *J. Hazard. Mater.*, 2006, 137:336-343.

[29] GUO C S, XU J, HE Y, *et al.*. Photodegradation of rhodamine B and methyl orange over one-dimensional TiO_2 catalysts

under simulated solar irradiation [J]. *Appl. Surf. Sci.*, 2011, 257:3798-3803.

[30] OCAMPO-PÉREZ R, SÁNCHEZ-POLO M, RIVERA-UTRILLA J, *et al*.. Enhancement of the catalytic activity of TiO_2 by using activated carbon in the photocatalytic degradation of cytarabine [J]. *Appl. Catal.* B, 2011, 104:177-184.

[31] RIVERA-UTRILLA J, SÁNCHEZ-POLO M, ABDEL DAIEM M M, *et al*.. Role of activated carbon in the photocatalytic degradation of 2,4-dichlorophenoxyacetic acid by the UV/TiO_2/activated carbon system [J]. *Appl. Catal.* B, 2011, 126: 100-107.

[32] LI G T, WONG K H, ZHANG X, *et al*.. Degradation of acid orange 7 using magnetic AgBr under visible light: the roles of oxidizing species [J]. *Chemosphere*, 2009, 76:1185-1191.

[33] YIN M C, LI Z S, KOU J H, *et al*.. Mechanism investigation of visible light-induced degradation in a heterogeneous TiO_2/Eosin Y/Rhodamine B system [J]. *Environ. Sci. Technol.*, 2009, 43:8361-8366.

[34] ZHANG N, LIU S Q, FU X Z, *et al*.. Synthesis of M/TiO_2 (M = Au, Pd, Pt) core-shell nanocomposites with tunable photoreactivity [J]. *J. Phys. Chem.* C, 2011, 115:9136-9145.

[35] ALKARAM U F, MUKHLIS A A, AL-DUJAILI A H, *et al*.. The removal of phenol from aqueous solutions by adsorption using surfactant-modified bentonite and kaolinite [J]. *J. Hazard. Mater.*, 2009, 69:324-332.

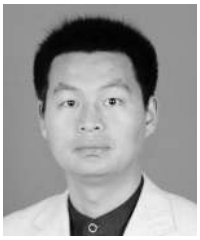

苗慧(1979 –),男,安徽太和人,博士研究生,2007 年于安徽师范大学获得硕士学位,主要从事功能材料合成及应用方面的研究。
E-mail: miaohuify@qq.com

崔玉民(1963 –),男,安徽亳州人,教授,1990 年于延安大学获得硕士学位,主要从事光催化等方面的研究。
E-mail: cymlh@126.com